

**RESEARCH INTO THE FURTHER DEVELOPMENT OF THE LIMPET
SHORELINE WAVE ENERGY PLANT**

SUPPLEMENT TO THE FINAL REPORT

ETSU V/06/00183/00/Rep

CONTRACTOR – WAVEGEN

The work described in this report was carried out under contract as part of the DTI Sustainable Energy Programme. The views and judgements expressed in this report are those of the contractor and do not necessarily reflect those the DTI.

First published 2003

© Crown Copyright 2003

1	Summary	3
2	Introduction	4
3	2D Testing	5
3.1	Methodology	5
3.1.1	Programme of tests	5
3.1.2	Power measurement and calibration	7
3.1.3	Incident sea power	8
3.2	Parametric study of water column performance	10
3.2.1	Optimum damping	10
3.2.2	Benchmarking the generic model	11
3.2.3	Water column surface length	12
3.2.4	Influence of front and rear wall slopes	13
3.2.5	Location along the horizontal plateau 5m water depth	17
3.3	Conclusions from 2D testing	21
4	3D Testing	23
4.1	Calibration and methodology.....	23
4.2	Programme of tests	24
4.3	Shoaling of wave power.....	24
4.4	Influence of coastline profile	25
4.5	Influence of device width.....	26
4.6	Comparison with narrow wave-tank tests.....	28
4.7	Influence of wave directionality	30
4.8	Analysis of wave energy contribution from each sea	30
4.9	Conclusions from 3D Testing	32
4.10	References.....	33

1 Summary

This report is supplementary to the main report for this project and describes a series of additional experiments. These were made using 2D and 3D models of shoreline OWC's at the facilities of the Queens University of Belfast. The purpose of the trials was to further investigate the geometric specification of shoreline OWC's , particularly the influence on hydrodynamic behaviour and power capture performance. The tests yielded the following conclusions which should be considered alongside the main report.

- Given a shoreline OWC device of a certain size and a fixed wave climate at the 20m contour, bathymetry has a much greater influence on device performance than changes to the device geometry. This highlights the importance of careful site selection and suggests that the precise choice of geometric sizes, provided they are within the range tested, will probably be dictated by other factors such as site constraints, structural design and construction techniques rather than performance.
- The performance of an OWC set in a reflective cliff is significantly better than that of the equivalent device in the open sea.
- Pneumatic power capture is not significantly reduced by directionally spread seas, or seas approaching at an angle to the shoreline.
- At the shoreline and in shallow water the high energy seas at the 20m contour make a much lower contribution to overall power capture than at the 20m contour because of energy losses through wave breaking and bottom friction. This means that a lower rated power conversion plant will be appropriate at the shoreline when compared with a similar nearshore unit.
- In a water-depth of five metres at the shoreline, an average pneumatic power of 1.3 kW/m^2 of water plane area can be obtained in an optimal configuration.

2 Introduction

Work performed and reported under the main body of the contract number ETSU V/06/00183/00/ highlighted a difference in the actual performance between the LIMPET shoreline oscillating water column wave energy generation plant installed on Islay and that predicted at the project initiation; the actual generation being significantly lower than expectation. One of the main reasons identified for the performance shortfall was the markedly different behaviour of the plant in the shallow water of the LIMPET site compared to the slightly deeper water used in the original model tests (the original bathymetric data available for the site at the time of project initiation proving to be erroneous). Retesting tank models with the site bathymetry correctly represented indicated a device performance which correlated well with site measurements and this led to the observation that in a site with deeper water at the shoreline the pneumatic power capture of LIMPET is likely to be as per the original expectation and to the question as to whether a collector chamber with an alternative geometry would perform better in the shallower water of the Islay site. In order to provide an answer to this question the scope of the Contract was extended to allow further tank testing to be performed on shoreline collectors with different geometries and under different bathymetric conditions.

The variables for consideration in the test programme included:

- Coastline profile
- Water depth at device mouth
- Bathymetry
- Incident wave spectra
 - Energy period
 - Incident wave energy flux density
- Collector width
- Slope angles
 - Front slope
 - Back slope
- Collector mouth height (Entry Gap)
- Collector beam at mean water level
- Dominant wave direction
- Wave directional spreading

A full matrix of possible parameter sets based on these variables was well beyond the available resource for the work and as such a baseline was selected with parameter excursions being made from the baseline.

The work was performed in the 2D and 3D wave tanks at the Queens University of Belfast under the direction of Professor T.J.T.Whittaker.

3 2D Testing

A series of experiments were performed in the 2D tank to investigate the generic influence of geometric parameters on the performance of an OWC collector. A prime objective of this work was to establish key results for reproduction in the 3D tank in the final stage of the project programme.

The main purpose of the study has been to explore the parameter map needed to design and estimate the performance of shoreline OWC wave power plant. The main geometric variables, which were investigated, included

- slope of the front wall of the collector (fw (deg))
- slope of the rear wall of the collector (bw (deg.))
- water column surface length from the front to the rear wall (L_o (m))
- vertical position of the lip of the front wall specified in terms of either
 - (d (m)) depth from the water surface
 - (LH (m)) lip height above sea bed
- water depth (h (m))

3.1 Methodology

In all the tests a seabed slope of 1 in 20 was used and the test model was placed on a horizontal plateau at various distances from the edge of the slope. Pneumatic power output from the models was calculated from the flow characteristics of an adjustable square orifice. The 2D tank at QUB is 0.33m wide and the tank floor was modified to give a 6m long section with a constant slope of 1:20 followed by a plateau 2.4m long. The same bathymetry was subsequently reproduced in the 4.5m wide 3D tank so that the wave shoaling process in both tanks was the same with the narrow tank representing a two dimensional slice of the wider facility.

All model configurations were tested in Bretschneider seas with the following characteristics to provide a spread of both wave periods and incident sea powers over a typical range found on a North Atlantic shoreline site (see table 1)

Energy period (Te) (s)	incident power (Pi) (kW/m)	Energy period (Te) (s)	incident power (Pi) (kW/m)	Energy period (Te) (s)	incident power (Pi) (kW/m)
7	15	10	15	13	40
7	40	10	40	13	65
		10	65		

Table 1

3.1.1 Programme of tests

The full programme of tests conducted in the narrow wave tank and the corresponding test numbers are presented in table 2.

Geometries							
Graph no.	Water depth	Collector mouth height		Water column	Front wall	Back wall	Description
QUB_-index	h [m]	(lip height)	(submerg.)	surface length	angle	angle	
		LH [m]	d [m]	L ₀ [m]	fw [deg]	bw [deg]	
13.03.03_004	5	2.5	2.5	6	70	40	optimum damped model, varying surface length
					70	40	
					70	40	
					70	40	
					70	40	
28.03.03_008	5	2.5	2.5	8	40	40	optimum damped model, varying front wall angle
					50	40	
					60	40	
					70	40	
					90	40	
13.03.03_009	5	1.5	3.5	8	40	40	optimum damped model, varying front wall angle
					50	40	
					60	40	
					70	40	
					90	40	
19.03.03_010	5	2.5	2.5	8	70	40	model moved along plateau (and slope) from -50m to +60m from the edge of the plateau
28.03.03_011	5	2.5	2.5	8	70	40	optimum damped model, varying back wall angle
					70	50	
					70	60	
					70	70	
					70	90	
20.03.03_003	5	1.5	3.5	8	70	40	comparison with LIMPET front face
		2.5	2.5	8	70	40	
		3.5	1.5	8	70	40	
20.03.03_012	5	2.5	2.5	7	70	60	optimum damped model, varying surface length
					70	60	
					70	60	
					70	60	
					70	60	
24.03.03_019	5	2.5	2.5	8	40	40	optimum damped model, parallel front and back walls
					50	40	
					60	60	
					70	70	
					90	90	
25.03.03_020 a-g	5	2.5	2.5	8	40 etc	40 etc	All Front Wall - Back Wall Angles For Te13 Pi65 And For Te10 Pi65 to Te7 Pi15
27.03.03_024	4	2.5	1.5	8	60	60	model moved along plateau at 0,8,10,20,40,60 [m]
28.03.03_025	6	4.5	1.5	8	60	60	model moved along plateau at 0,8,20,40,60 [m]
28.03.03_026	8	4.5	3.5	8	60	60	model moved along plateau at 0,8,20,40,60 [m]
31.03.03_028	10	4.5	5.5	8	60	60	model moved along plateau at 0,8,20,40,60 [m]
07.04.03_029	all	all	all	8	60	60	model in different water depths
08.04.03_029	all	all	1.5	8	60	60	model in different water depths
29.04.03_031	10	6.5	3.5	8	60	60	model moved along plateau at 0,8,20,40,60 [m]
29.04.03_032	10	all	all	8	60	60	model with different lip depths

Table 2: 2D-tests and parameters studied

3.1.2 Power measurement and calibration

3.1.2.1 Orifice calibration

Previous experiments on LIMPET have shown that the cyclic performance of the device was not significantly different when the column was damped using a linear damper compared to an orifice. For convenience it was thus decided to use an adjustable double 'V' notch orifice for the parametric tests. Also, as the slopes of the front and back walls in the models were changed over a significant range, together with the often complex shape of the water column surface profile, it would have been difficult to measure the movement of the water column surface using wave probes.

Power damping calibration factors were used in conjunction with R.M.S. (root mean square) pressure in the plenum chamber to calculate power. Relationships between power damping and R.M.S. pressure were determined for square orifices with a diagonal opening of between 10 and 50mm in 5mm steps and in 1mm steps between 15 and 25mm. The finer increments were needed to determine the optimum damping for each geometric configuration tested and therefore ensure that any variation in power output in a given sea was due solely to changes in water column geometry.

The orifices were calibrated using a 'U' tube part filled with water and oscillated by means of a piston in one limb and damped using the orifice on top of the other to produce different water column strokes. *Figure 1* shows the relationship between damping (N.s/m^5) and R.M.S. pressure for a 22mm orifice opening. The curve fits for a range of orifice openings, are shown in *figure 2* for a range of openings.

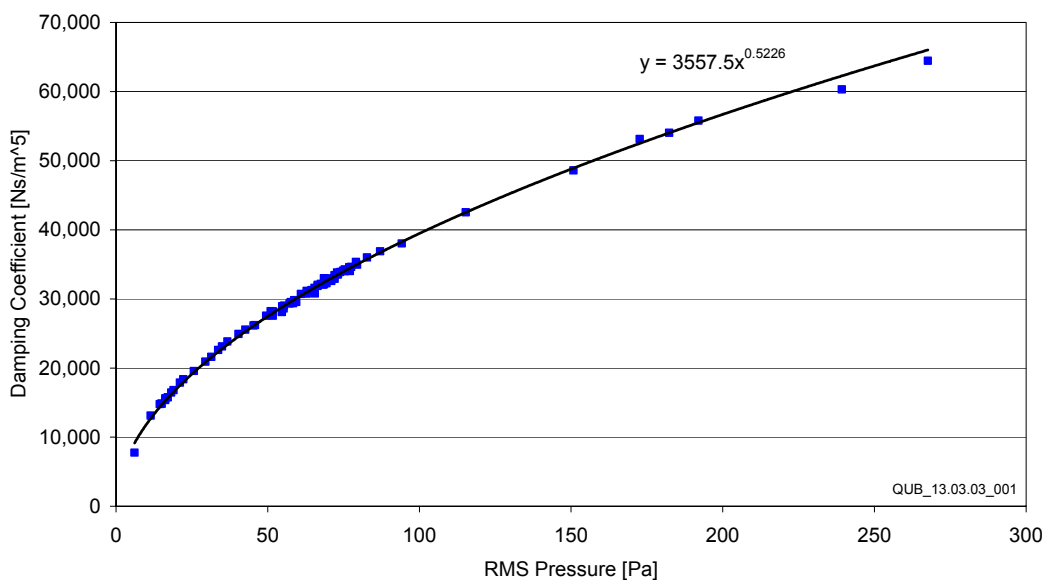


Figure 1: Calculation of damping from pressure for an orifice opening of 22mm

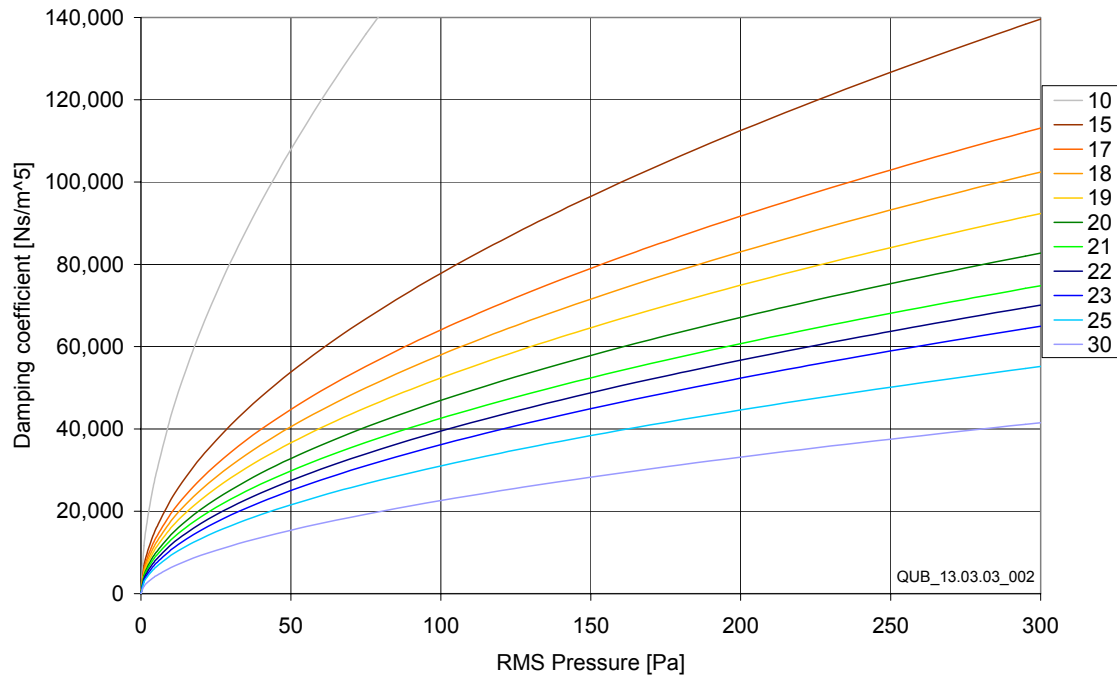


Figure 2: Damping - curve fitting for different orifice openings

3.1.2.2 Pneumatic power calculation

The pneumatic power measured in the experiments was calculated in two ways from the time series and compared. In the pressure time series the zero up crossing and down crossing was identified and the R.M.S. pressure calculated for each cycle. From the orifice relationships the damping was calculated for each part cycle and the power calculated from $(\text{R.M.S. pressure})^2/\text{damping}$ and then summed over the complete scan period. The output of this calculation was compared with the power calculated using the R.M.S. pressure for the complete time series and one value of damping. In general the values calculated were within 5% of each other with the latter method giving the higher value.

3.1.3 Incident sea power

During the programme of experiments the plateau at the end of the seabed slope was set at a scale depth of 4,5,6,8 and 10m. This was achieved by moving the bed of the tank. The sea power was calculated at each 1m contour along the seabed slope as well as along the plateau for each water depth. A summary of the results obtained is presented in **figure 3** for the range of Bretschneider seas used. **Figure 4** shows the sea power when the plateau is set at 5m depth and **figure 5** is for a plateau depth of 10m. In all these figures the x-axis is split with the first part giving the depth contour across the seabed slope and the latter part giving the distance along the plateau measured from the top of the slope. **Figure 4** (plateau depth 5m) clearly shows the effect of wave shoaling and energy loss due to breaking particularly in the higher powered seas. The drop in incident sea power along the plateau is also very evident. In

comparison *Figure 5* (plateau depth 10m) shows relatively little loss in sea power with both depth and distance along the plateau.

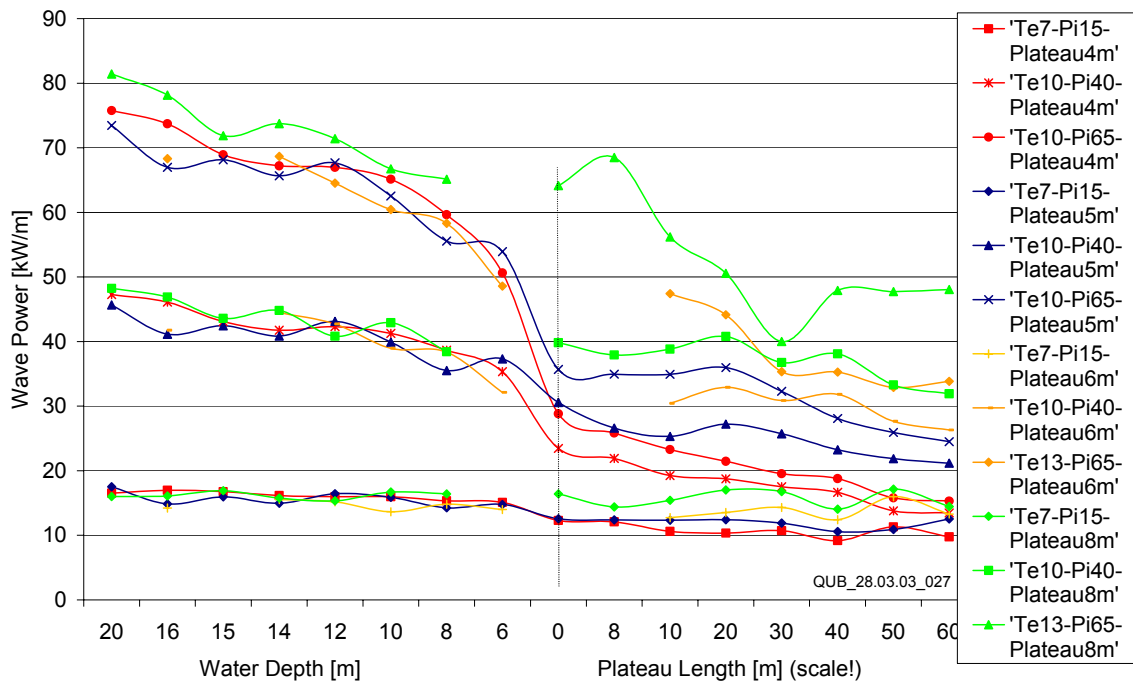


Figure 3: Wave power along slope and different water depths at the plateau

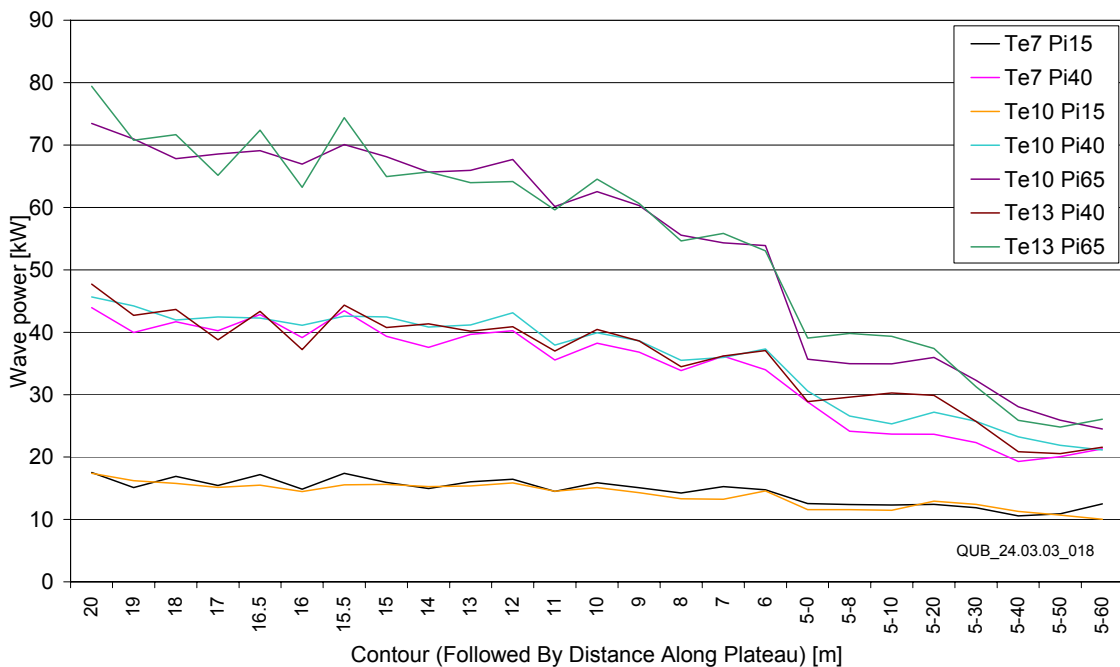


Figure 4: Changing wave power at different contours for the 5m plateau depth

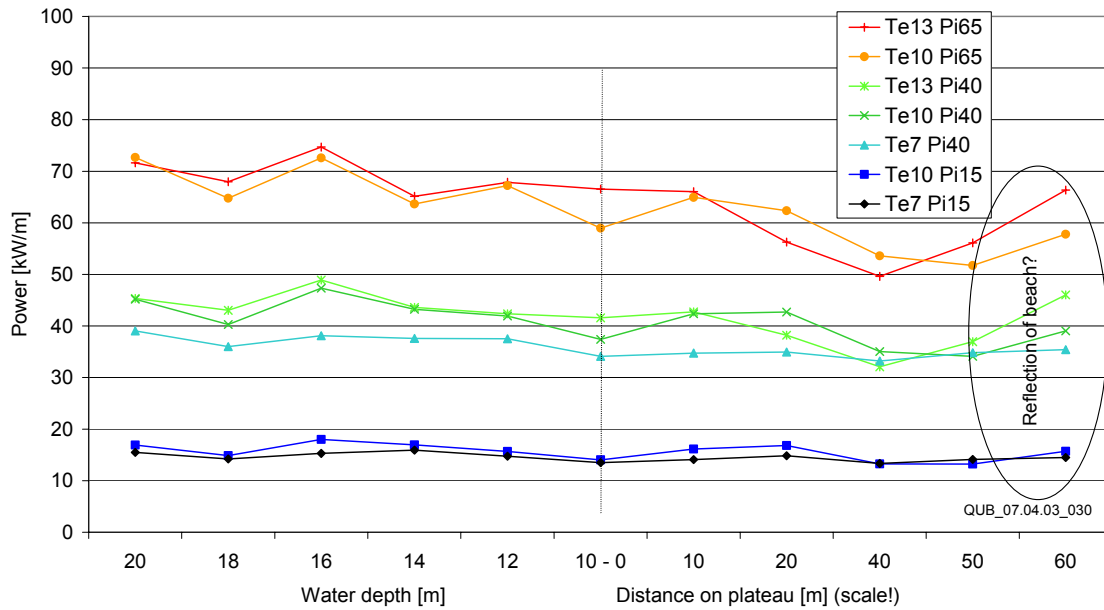


Figure 5: Wave shoaling in 10m water depth

3.2 Parametric study of water column performance

3.2.1 Optimum damping

Previous experience of testing OWC plant during the past 25 years had clearly shown the importance of optimising the damping of the water column in each test in order to ensure that changes in performance are due solely to variations in column geometry. **Figure 6** shows the results of a typical optimum damping test carried out with each geometric configuration. Here the x-axis is a measure of the orifice opening at model scale. It should be noted that this can be converted to water column damping at full scale but orifice opening provides an easily recognised parameter for comparing results from test to test. Shallow water OWC's are not particularly sensitive to damping provided the level is in the correct general range. In the case presented, orifice openings of between 19 and 25mm do not affect performance significantly in random seas. This range of orifice openings equate to damping levels of between $20,000\text{Ns/m}^5$ and $45,000\text{Ns/m}^5$. In general it is better to be over damped rather than under damped as excessive column motion leads to turbulent losses around the front lip, with a more rapid deterioration in power capture.

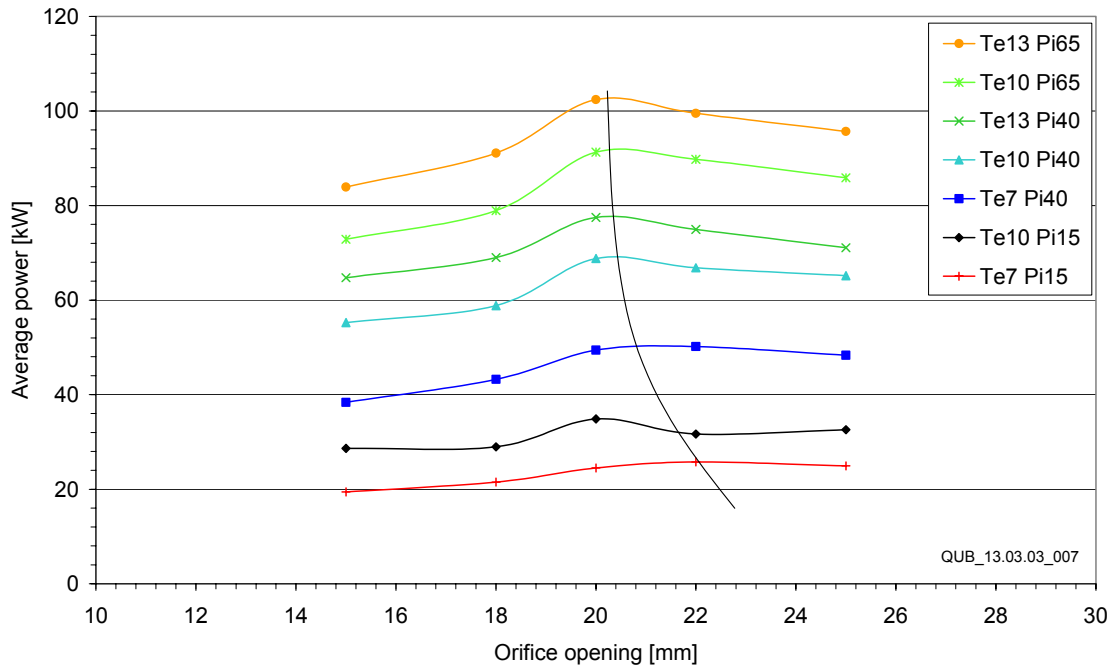


Figure 6: Plain wall model with fw/bw 70°/40° in Bretschneider seas (h 5m, surface length 8m, lip submergence 2.5m)

3.2.2 Benchmarking the generic model

The generic model manufactured to conduct the test programme comprised straight front and back walls of constant thickness. It was important to benchmark the tests by configuring the generic model in a way which represented other geometries which had been tested previously. Consequently a significant proportion of the parametric study of the geometric variables defining the water column was conducted at a depth of 5m as this correlated with the mean tide level at the LIMPET plant and is typical of several coastline sites. Initially front and back wall angles of 70 and 40 degrees with a horizontal spacing of 8m at still water level was used, as it was the closest configuration to the LIMPET plant. In this series of tests the front wall lip submergence depth was varied from 1.5 to 3.5m. In addition a set of tests was performed with the plain front wall of the generic model replaced by the more complicated sectional profile of the LIMPET front wall. The model was normally located 8m from the edge of the plateau except in the test series to look at the effect of plateau length. The model tests were conducted at a nominal scale of 1 in 40 and all the results presented are at full scale unless it is indicated to be otherwise in specific instances. In the narrow tank the water column tested was 7m wide, which is 53% of the tank width.

Figure 7 presents the average pneumatic power in the full range of seas tested, in histogram format. Each pair of bars compares the generic model with the LIMPET front wall model. In general there is relatively little difference between the paired configurations. **Figure 7** shows that the 3.5m deep front wall lip significantly reduces pneumatic performance, whilst performance with 2.5 and 1.5 m submergence are relatively similar. In the tests with the shallowest lip and the medium and high powered seas the lip occasionally broke free of the water surface in the largest waves

in the sequence reducing the plenum chamber pressure to atmospheric for part of the wave cycle. This loss of power was compensated for by an increase in energy transfer from the wave to the column giving similar output for the 1.5 and 2.5m lip depths. A further observation was that the pneumatic power was greater at the higher values of energy period. The pneumatic power was the highest with a T_e of 13s compared to 7 and 10s even with the same incident sea power.

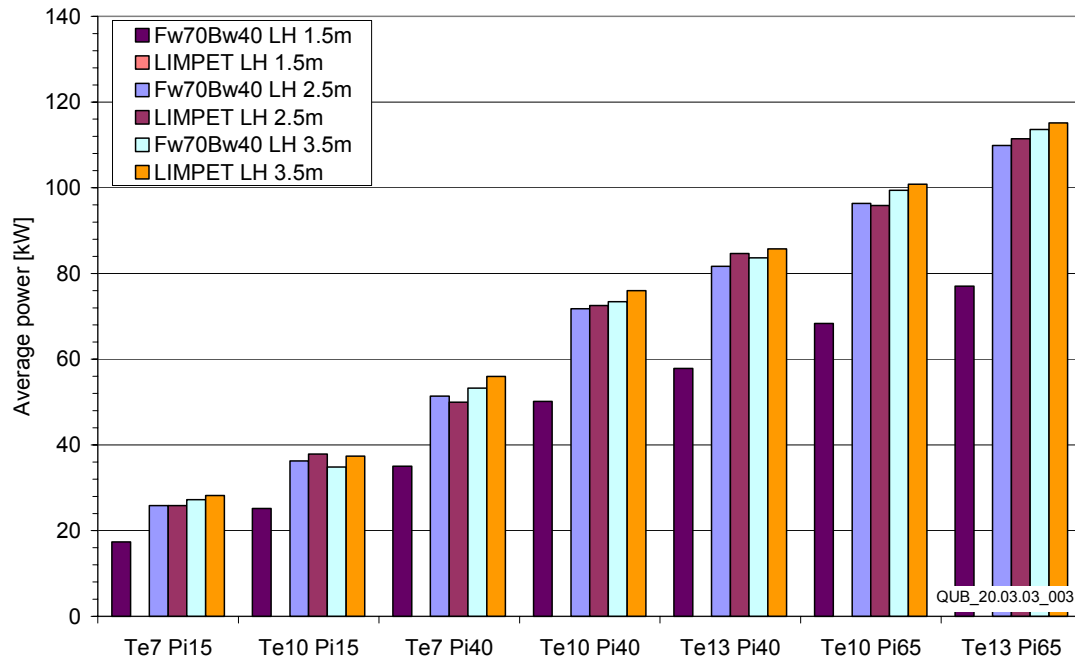


Figure 7: Optimum damped model in Bretschneider seas (surface length 8m, h 5m)

3.2.3 Water column surface length

Figure 8 shows the relationship between the average pneumatic power in the range of seas tested as a function of water column length. The results for the LIMPET front wall configuration are shown also and are in close agreement with those from the generic model with a water column length of 8m. In general there is an increase in pneumatic power as the water column surface length is increased from 6 to 11m. 11m was chosen as a practical upper value for length due to the increasing cost of the structure with size. It is expected that the pneumatic power would not continue to increase with length as secondary waves on the water column surface become more energetic and the column tuning varies. Although the T_e 13/ P_i 65 sea indicates a 10% increase in pneumatic power when the length is varied from 8 to 11m there is very little difference with the lower energy seas. This is an important as these seas are the most commonly occurring and it is not necessarily cost effective to provide the necessary M&E plant to cope with the infrequent large seas.

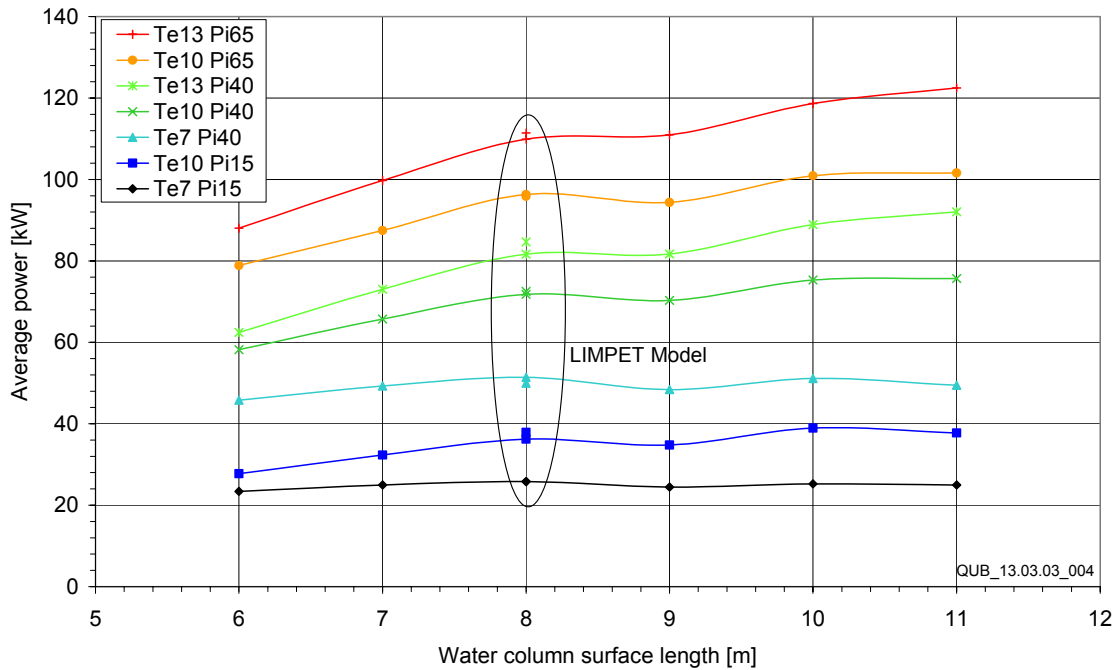


Figure 8: Optimum damped model in Bretschneider seas (Lip submergence 2.5m, plain walls: fw/bw 70°/40°, h 5m)

Consequently it is concluded that a water column surface length of 8 to 10m is a reasonable compromise and confirms the choice of 8m in the LIMPET plant.

3.2.4 Influence of front and rear wall slopes

Figures 9 a to g show the average pneumatic power in the range of seas tested with different front and back wall angle combinations. The x-axis gives front wall angle and the data points are drawn for the range of rear wall angles specified. The spread of pneumatic power measured was + or – 10% from the mean value of the maximum and minimum power level for the data set with the Te7 / Pi15 sea increasing to + or – 12% in the Te13 / Pi65 sea. Therefore, sea state has relatively little effect on the range. In all cases, irrespective of slope, columns with parallel front and rear walls gave the best performance. Walls inclined at 60° to the horizontal gave marginally better performance than those at 70°.

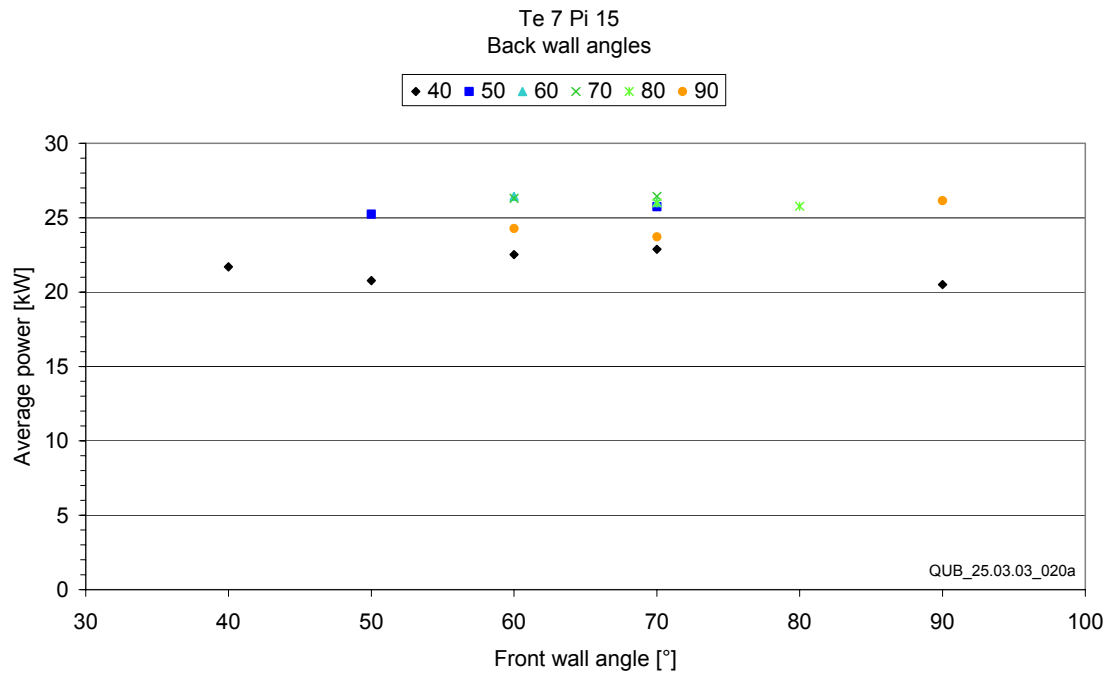


Figure 9a

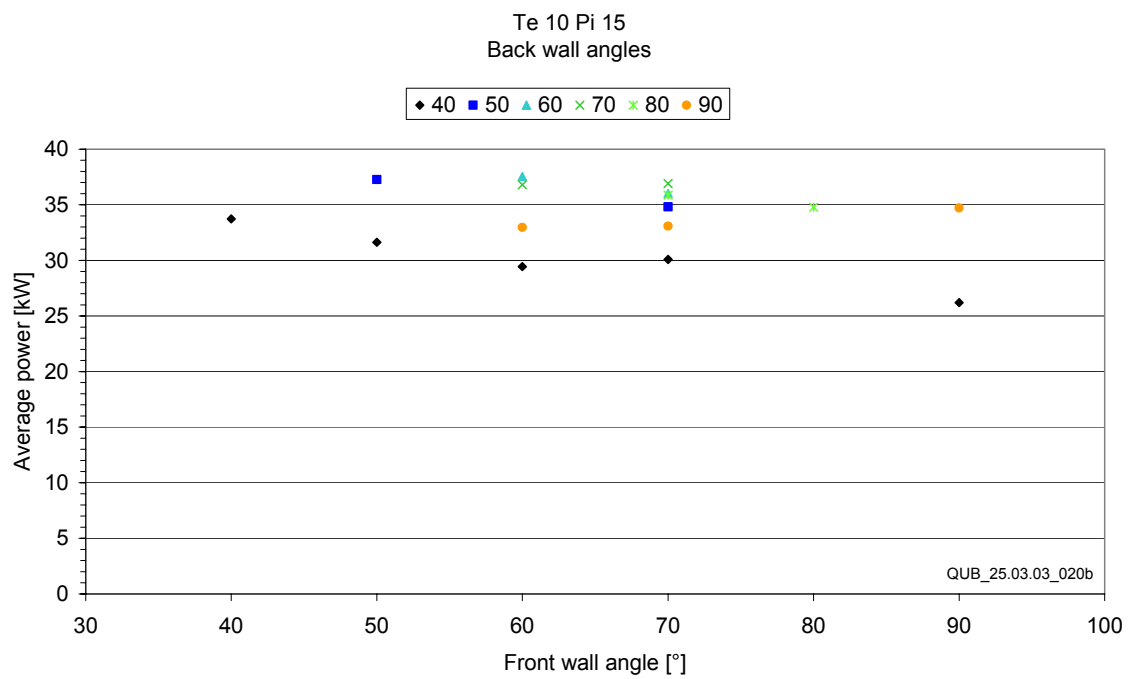


Figure 9b

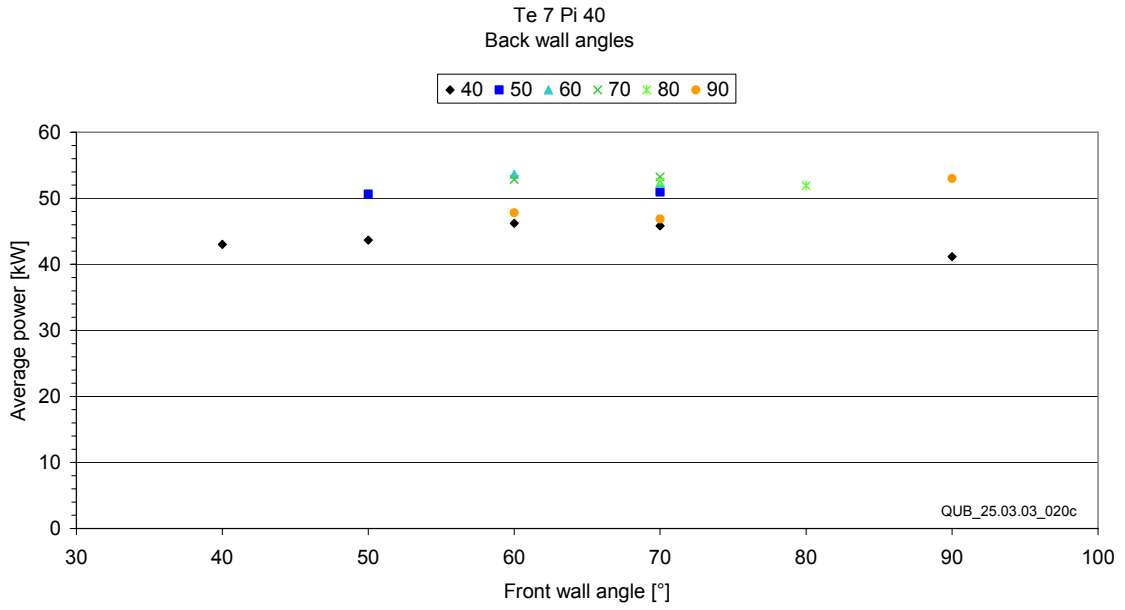


Figure 9c

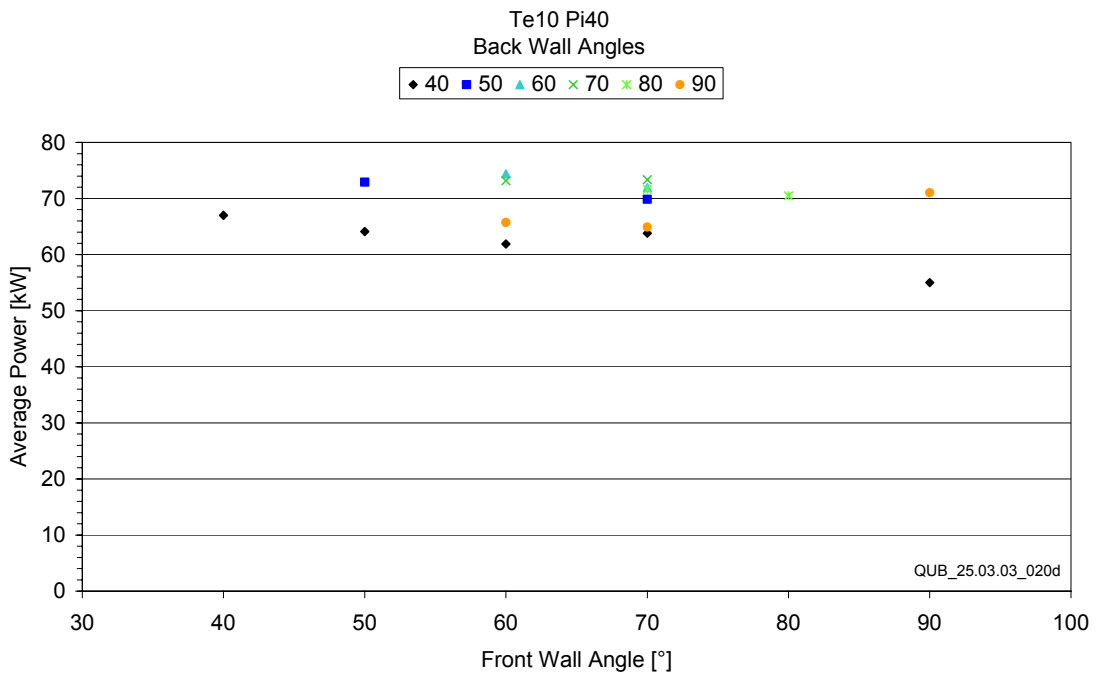


Figure 9d

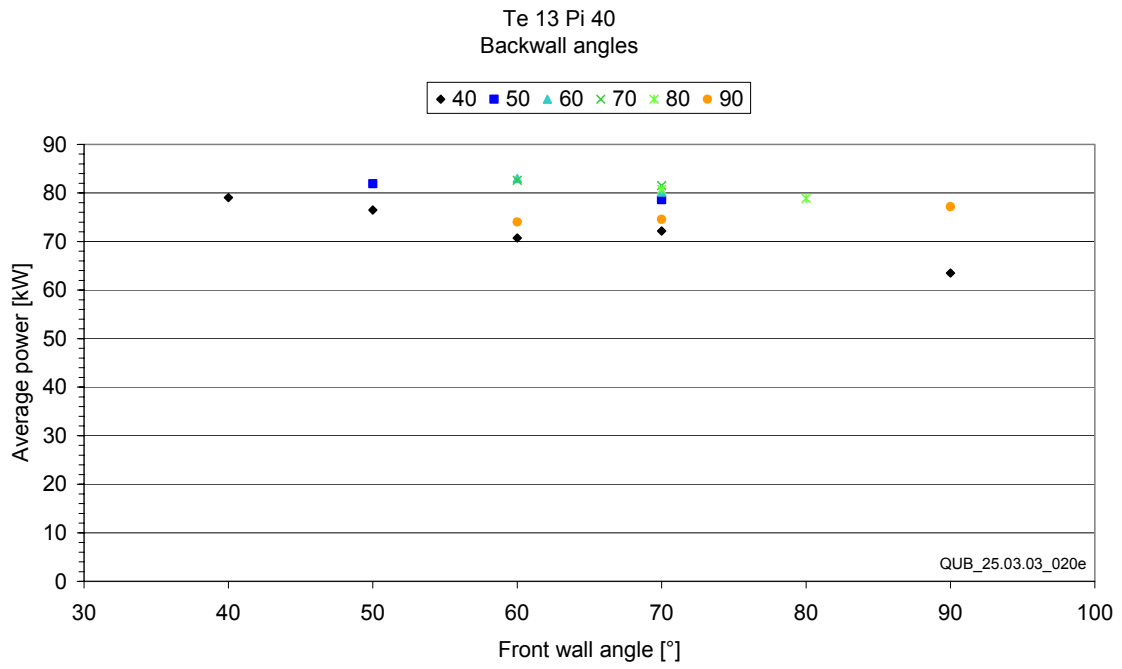


Figure 9e

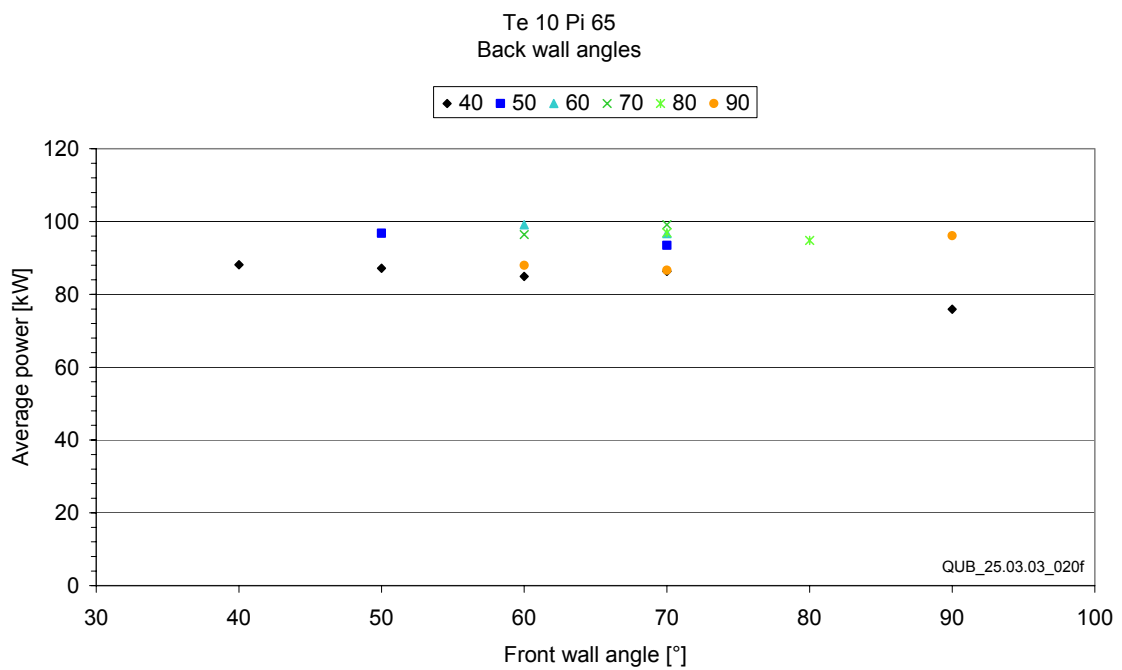


Figure 9f

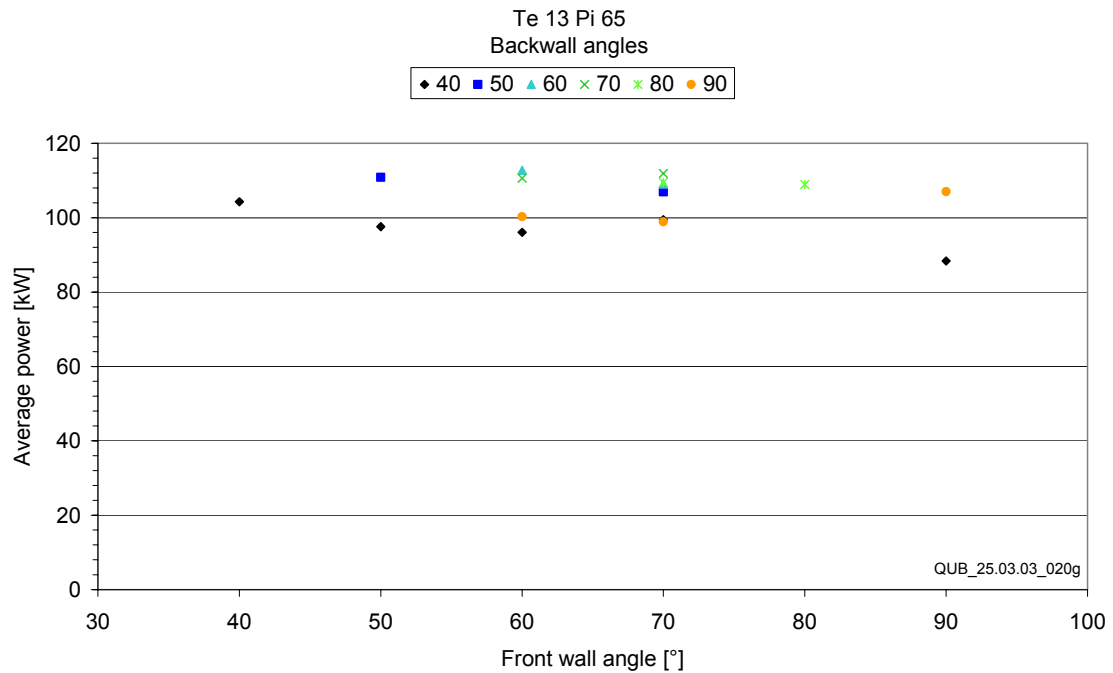


Figure 9f

Figures 9 a – g: Front and back wall angle combinations (water depth 5m, lip submergence 2.5m, surface length 8m)

3.2.5 Location along the horizontal plateau 5m water depth

The section on incident sea powers showed the significant reduction in wave energy with water depth and distance along the plateau. The model with front/back wall angle 70/40 degrees, lip depth 2.5m and water column surface length 8m was used to ascertain the variation in pneumatic performance with position along the plateau and in different water depths. A plateau depth of 5m was used. **Figure 10** shows the variation in pneumatic power as a function of horizontal location in the range of seas tested. Taking the leading edge of the plateau as the reference point moving 60m back resulted in a reduction in pneumatic power of 43% in the largest seas reducing to 12% in the smallest.

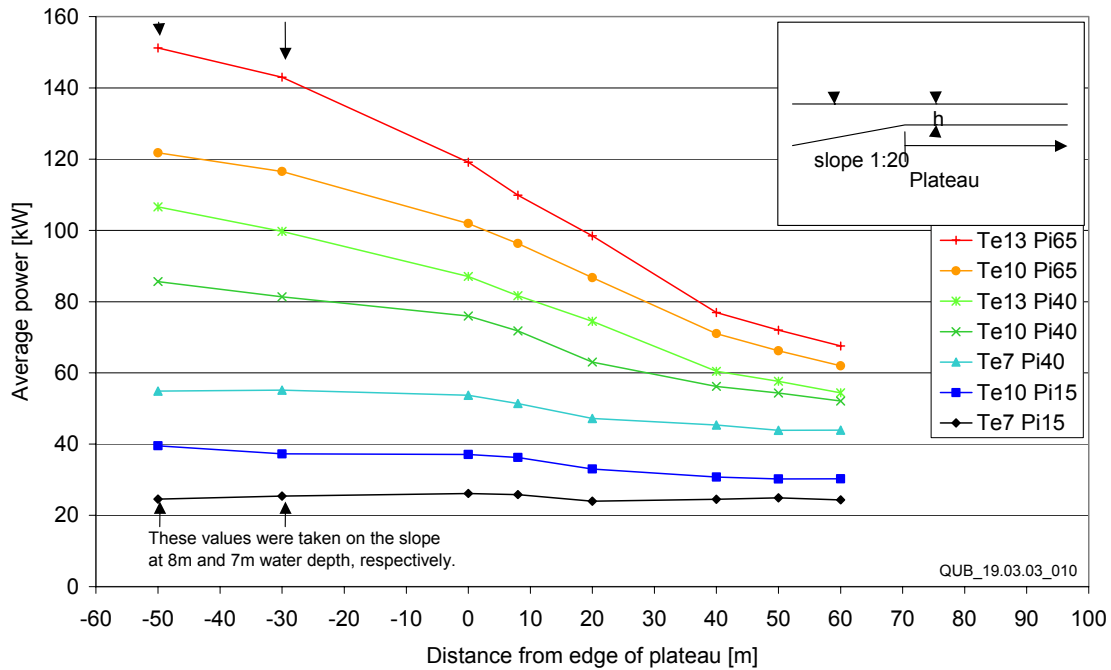


Figure 10: Optimum damped model in Bretschneider seas (fw/bw 70°/40°, surface length 8m, h 5m, lip depth 2.5m)

The consequence of this observation is that position along the plateau has a significant effect on the required capacity of the M&E plant as the maximum pneumatic power is significantly reduced in the largest most energetic seas. Thus the wave power device is naturally protected with a natural limitation of the energy in the storm waves reaching the plant.

It is interesting to note that if the incident sea power in the Te10/Pi65 and Te10/Pi40 seas at the front wall, taken from *figure 3*, is compared with the pneumatic power measurements in the same seas taken from *figure 10* the capture factors are 35% and 34% respectively. When the capture factor is calculated using the sea power at the 20m depth contour the values are dramatically reduced to 12% and 16.5% respectively. *Figure 10* also shows the performance of the 70/40 column located on the sea bed slope at depths of 8 and 7m. In the seas tested the pneumatic power tested at 8m water depth ranges from 25kW in the (Te7/Pi15) sea to 150kW in the (Te13/Pi65) sea giving capture factors of 26% and 21%. In the same seas the device located 60 from the edge of the 5m deep plateau gives capture factors of 12% and 20% respectively. Consequently this data indicates that if the current LIMPET plant were moved from its current position to a location where the depth was 8m at the cliff face without a plateau the peak pneumatic power would be increased by 220%.

A series of tests were conducted with plateau depths of 10m, 8m, 6m and 4m. A model with front and rear wall slopes of 60° and a water column surface length of 8m was used. *Figures 11, 12, 13 and 14* show the average power in the range of seas tested for plateau depths of 10, 8, 6 and 4m respectively. These curves show that location along the plateau becomes less significant as the water depth is increased even with the larger seas.

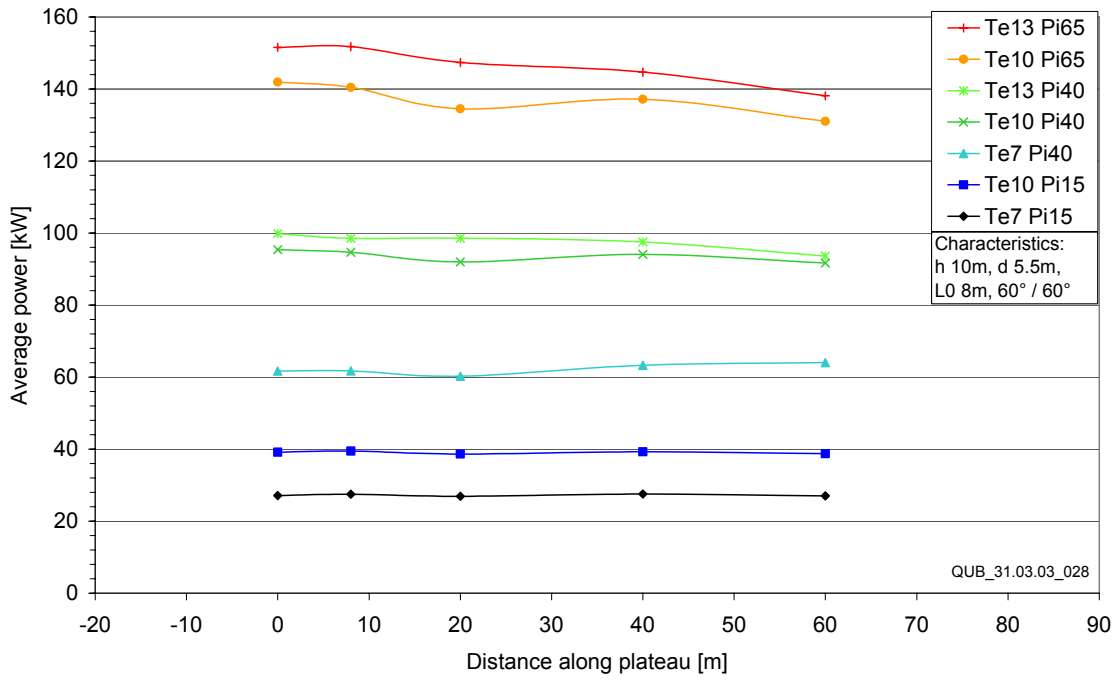


Figure 11: Optimum damped model located along the plateau in 10m water depth

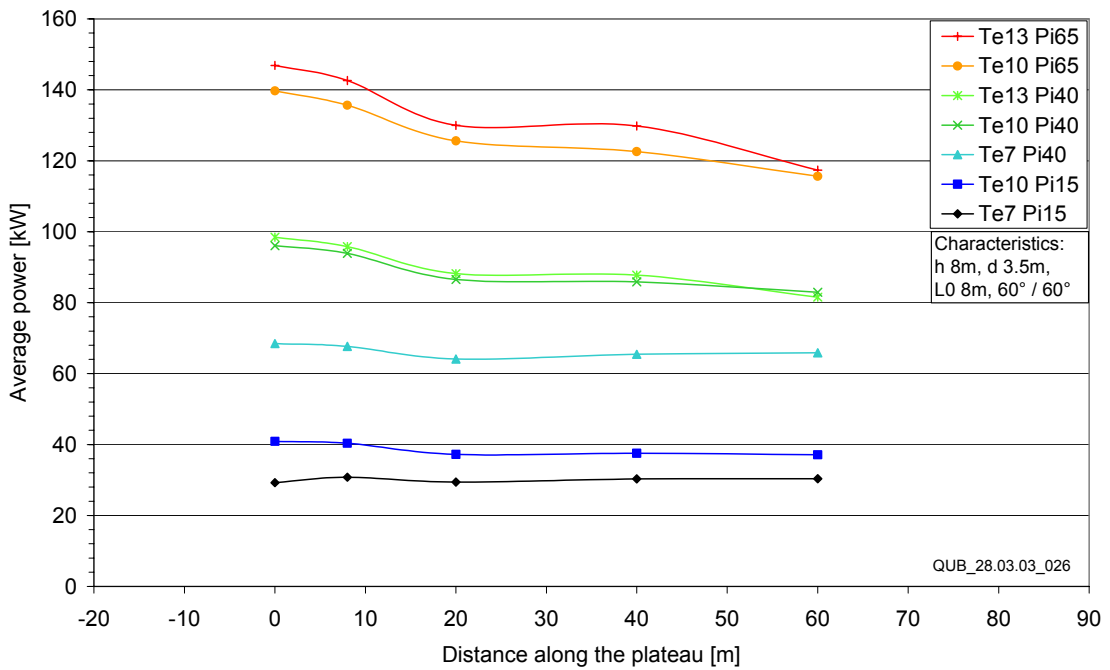


Figure 12: Optimum damped model located along the plateau in 8m water depth

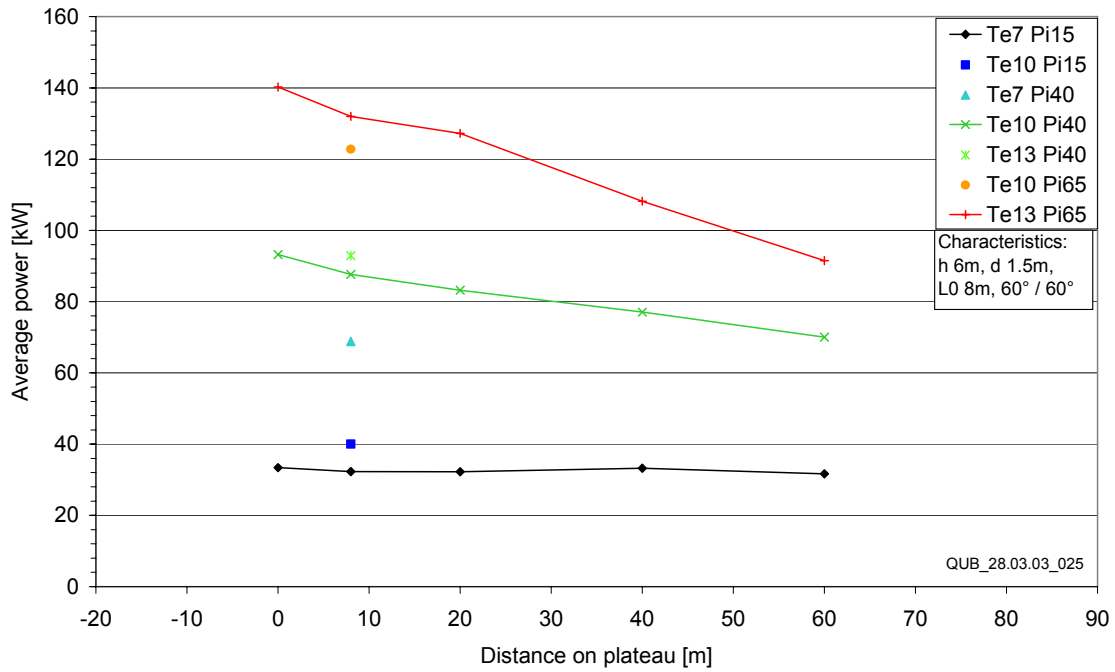


Figure 13: Optimum damped model located along the plateau in 6m water depth

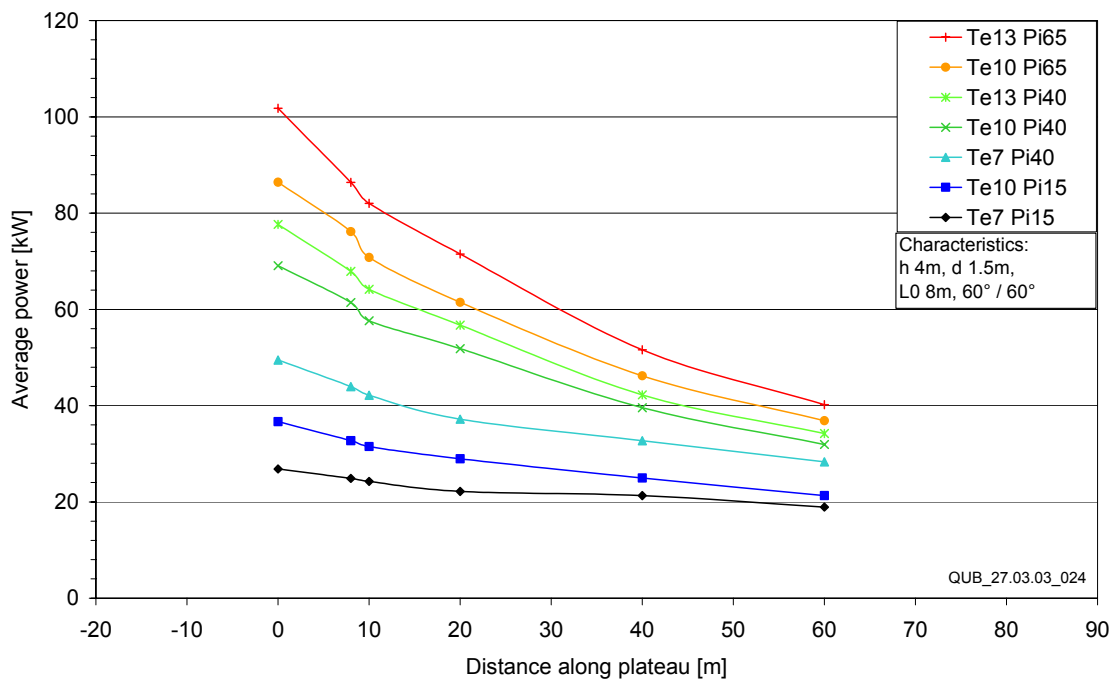


Figure 14: Optimum damped model located along the plateau in 4m water depth

Examination of the results shows that, in this study, the most significant parameter effecting pneumatic performance is distance along the plateau particularly in the shallowest water depths combined with the largest seas. In a water depth of 4m the reduction in pneumatic performance over the 60m length of the plateau ranged from 39% to 29% from the largest to the smallest seas tested compared to a range of 15% to 0% reduction for 10m depth.

Figure 15 summarises the influence of water depth on average pneumatic power capture for all of the test seas. This figure clearly illustrates the reduction in power capture with water depth, which is especially significant for high energy seas.

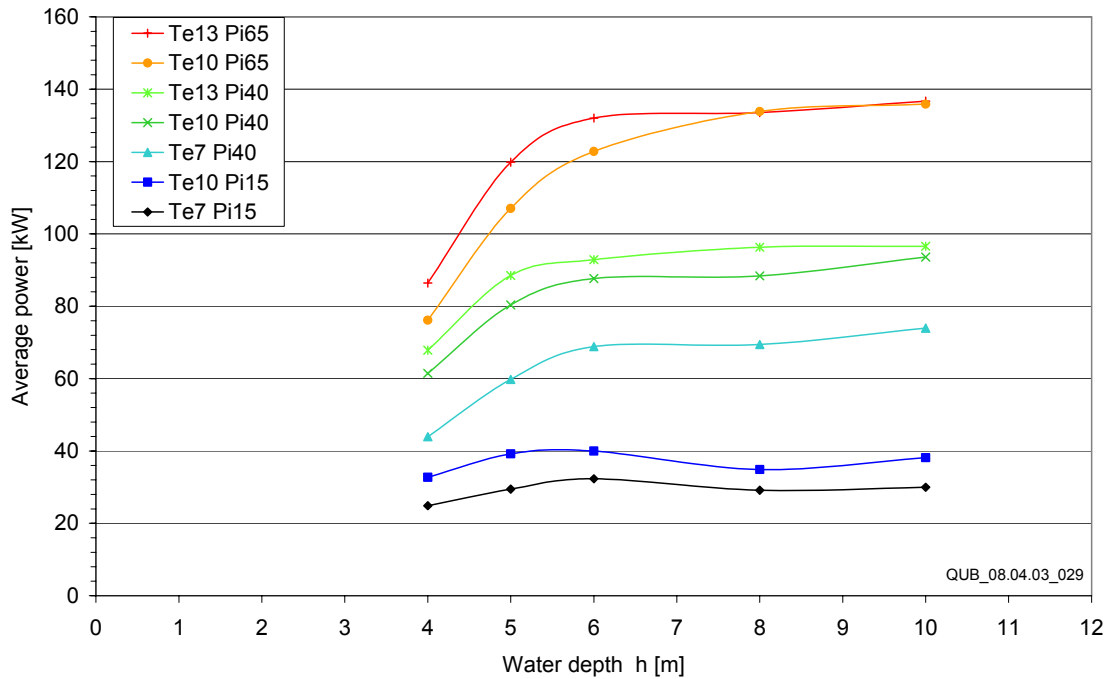


Figure 15: The 60°/60° model in different water depths (located at 8m on the plateau, L_0 8m, d 1.5m)

3.3 Conclusions from 2D testing

The series of tests conducted in the narrow wave tank have yielded a number of significant conclusions.

1. Water depth and shoaling are the most significant factors effecting pneumatic performance.
2. In very shallow water (4m) the presence of a horizontal plateau significantly influences capture and should be avoided if possible. In deeper water (10m) or more the effect is much less significant.
3. The models are relatively insensitive to applied damping with only a 5% variation in power when varied from the optimum value to twice the level.
4. The water column is relatively insensitive to front and rear wall slopes with the maximum variation being $\pm 12\%$ over the complete geometric range tested. In general parallel front and rear walls, with a slope of 60° to the horizontal, gave the best performance.
5. Shallow lip immersion depth (1.5m) is best, although the lip can break free of the water surface in the largest wave troughs causing rapid pressure fluctuations.

6. Performance increased when the water column surface length was varied from 6 to 11m in 1m increments. With greater lengths there was a notable increase in parasitic waves on the water column surface. Lengths of between 8 and 10m offer the best compromise.
7. In this type of shallow water wave power device, the precise choice of geometric sizes, provided they are within the range tested, will probably be dictated by other factors such as site constraints, structural design and construction techniques rather than performance.

4 3D Testing

On completion of tests in the 2D tank a number of the parametric combinations examined were tested in the 3D tank to establish any influence of width limitation and the presence of reflective walls. In addition the wide tank was used to examine parameters that could not be examined using the narrow wave-tank, namely:

- Incident wave directionality
- Coastline profile
- Water column width

Further to the parametric analysis, the relative significance of each test sea was estimated. A weighting was applied to each test sea, equal to its annual probability of occurrence at a site on the west coast of Scotland, derived from data from Waverider buoy 62106 (http://www.ndbc.noaa.gov/Maps/United_Kingdom.shtml).

4.1 Calibration and methodology

The wide wave-tank has been calibrated to produce seas with similar incident wave energies at the 20m contour to those produced in the narrow wave-tank. The same Bretschneider function was used to produce the spectral distribution. However, exactly the same incident wave power is not produced and so comparisons between the narrow and wide wave-tanks are obtained by using capture factors.

Directional seas are obtained by varying the peak wave direction, θ_p , and the spreading parameter, s , where $S(f,\theta) = S(f)\cos^{2s}\theta$, as shown in the table below. This cosine-squared spreading function is commonly used for wave climates (Demirbilek & Vincent 2002). These values were generally used with all seven of the test seas.

Peak wave direction	Spreading parameter
0°	Infinite
0°	15
15°	Infinite
15°	15

N.B. an infinite spreading parameter equates to a long-crested (plain) wave

Unless stated otherwise the same methodology for the tests performed in the narrow wave-tank was used for the testing in the wide wave-tank. Similarly, the methods for damping optimisation and pneumatic power calculations used in the previous analysis of results were used.

To limit the number of tests required the angle of the chamber front wall and the angle of the back wall have been kept constant for these tests and equal to the optimum angles identified in the narrow wave-tank tests. These are a front wall angle of 60° and back wall angle of 60°. The optimum lip submergences of 1.5m for a water depth of 5m and 2.5m for a water depth of 8m are used for these tests.

4.2 Programme of tests

The following tests were conducted in the wide wave-tank at QUB

Test set	Water depth	Device width	Water Surface length	Coastline	Notes
WWT001	5m	7m	11.4m	Plain	
WWT002	5m	10m	8.0m	Plain	
WWT003	5m	12m	10.0m	Plain	
WWT004	5m	12m	6.7m	Plain	
WWT005	5m	10m	8.0m	Absorbing	
WWT006	5m	10m	8.0m	Headland	
WWT007	5m	10m	8.0m	Gully	
WWT008	5m	-	-	-	Shoaling experiments
WWT009	8m	8m	10m	Plain	
WWT010	8m	10m	10m	Plain	
WWT011	8m	12m	10m	Plain	

4.3 Shoaling of wave power

By way of confirmation, the results of shoaling experiments shown in *Figure 16*, illustrate that the effect of water depth on power capture have been modelled similarly in both the narrow and wide wave-tank.

It can be clearly seen that the more energetic seas are significantly reduced by shoaling, whilst the less energetic seas ($P_i < 20 \text{ KW/m}$) do not lose much energy. This energy loss is largely associated with wave breaking and could be observed clearly during the shoaling tests. This loss of energy from the more energetic seas looks dramatic and could be expected to significantly reduce incident power, however whilst there is a reduction in average incident power it is not as significant as Figure 1 suggests. This is because typically, for more than 60% of the time (using data from the 62106 Waverider buoy), the incident wave power is less than 20 kW/m, which is not significantly reduced by shoaling down to a water depth of 5m. The significance of any analysis must be taken into consideration by considering its likelihood of occurrence. This is dealt with further in **Section 4.8**.

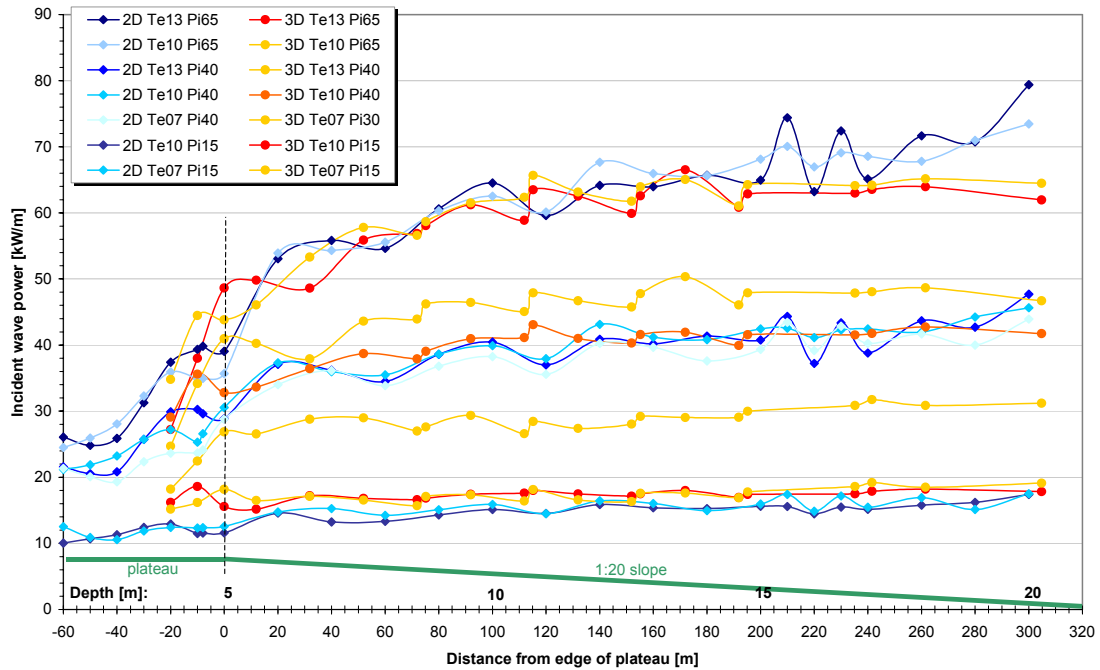


Figure 16: Comparison of shoaling effects for the narrow and wide wave-tanks at QUB

4.4 Influence of coastline profile

The 10m wide model with 80m² water plane area was used to examine the effect of the coastline profile in 5m of water. Three different coastline profiles were tested.

Profile 1: Model set in gully in coastline

Profile 2: Model set in linear coastline

Profile 3: Model set on promontory in coastline

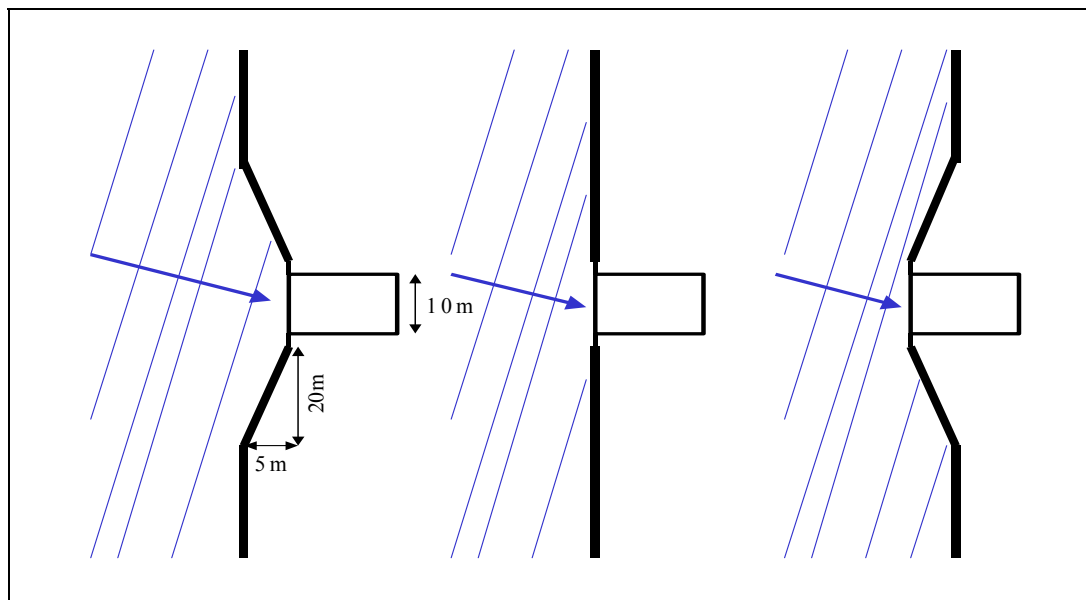


Figure 17: The three coastlines

In testing, the coastline was built around the model using smooth concrete blocks, with the model always placed 10m back from the edge of the plateau so that all

coastlines could be wholly constructed on the plateau. The three coastlines are shown in *Figure 17*. Comparison of the power capture for the three coastlines is shown in *Figure 18*.

The effect of the coastline profile can clearly be seen where for all seas the pneumatic power is increased for a gully and decreased for a headland. This confirms previous results, which have shown an increase in power capture in a flared gully, due to the waves being funnelled into the water chamber (Stewart 1993).

It may have been expected that the power capture would also increase for a headland due to an increase in wave height that is typically predicted by diffraction models to occur at headlands. However, unlike the wave-tank model, an actual headland would have an associated bathymetry extending out into the ocean. It is this bathymetry, which causes the increase in wave height on a headland, not the headland itself.

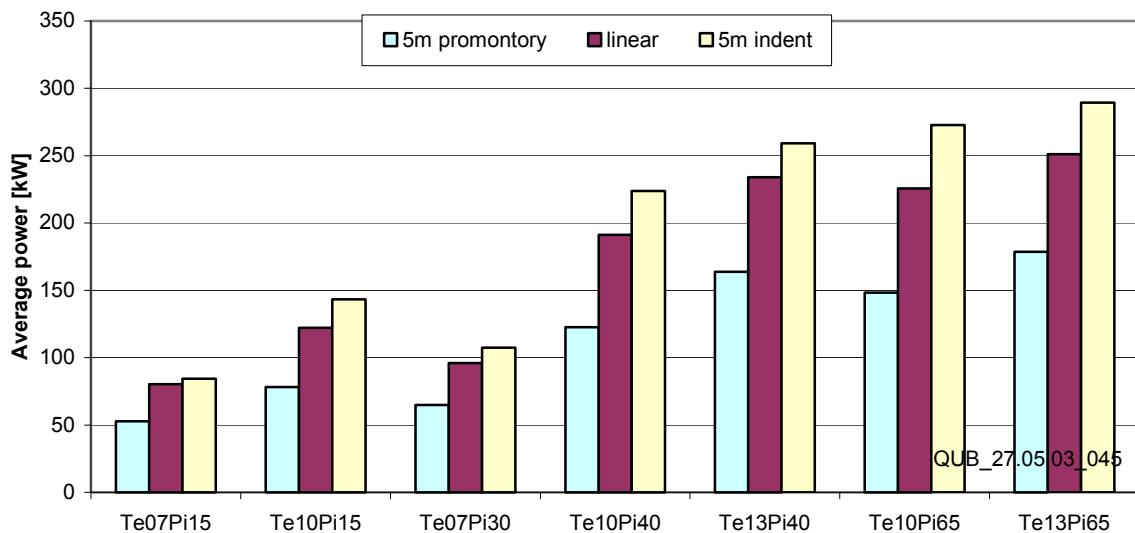


Figure 18: Comparison of pneumatic power for different coastline profiles

A corollary of this influence of bathymetry suggests that increases in performance due to the use of a natural gully, where the waves are funnelled into the water chamber, need to be slightly decreased to account for the de-focusing of waves in a gully (although it would be expected that this effect is smaller than the funnelling effect).

The positioning of a device on a headland also means that the waves will not so readily build up at the mouth of the water column chamber, resulting in a reduction in power capture as illustrated from the results shown in *Figure 18*. This can be viewed as the converse effect to a gully, with waves being dispersed away from the mouth of the water chamber.

4.5 Influence of device width

The influence of device width on pneumatic power has been investigated using two different procedures to highlight two different aspects of device width. Tests done in a water depth of 5m involved changing the device width whilst maintaining a constant water-column water plane area of 80 m². The wave force on an oscillating water column is approximately proportional to its wave plane area and for a small device, viz. point absorber, the power capture will be equal to the product of the wave force

and column velocity in-phase with this wave force. Thus, assuming that the dynamics do not change, the power capture will be proportional to the water plane area. By keeping the water plane area constant the effects of changing the device width can be more easily isolated from the more dramatic changes due to changing the water plane area. Thus, these tests illustrate the relative effects of device width on performance. Tests done in a water depth of 8m involved changing the device width whilst maintaining a constant water surface length of 10 metres (approximately the same water surface length as LIMPET, which was 9.3m). These results help to illustrate the absolute influence of device width on performance. The choice of water depth for each set of tests was arbitrary, the tests in two depths being used to determine whether performance relative to directionality is influenced by water depth.

The results of tests performed in 5m water depth to investigate the relative effect on performance of device width are shown in **Figure 19**. Although there is some small variation in pneumatic power capture there is no strong influence on performance due to device width. It is postulated that this is because even for the widest model tested, the device width is still only a small proportion of a typical wavelength. Thus large transverse waves in the water chamber do not develop and so energy is not lost through this mechanism.

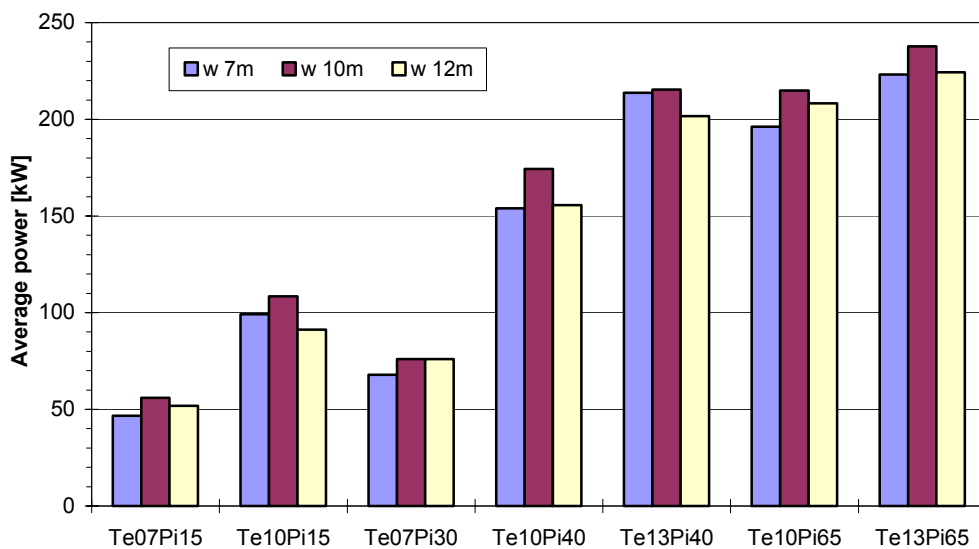


Figure 19: Influence of device width on pneumatic performance whilst maintaining a constant water plane area

The results of experiments, with a water depth of 8 metres and varying the device width whilst keeping all other parameters constant, are shown in **Figure 20**. These show that in the higher power tests, $P_i > 30$ kW/m, the power capture increases approximately proportionally to the device width, or perhaps more accurately proportionally to water plane area. However, in the lower power tests, $P_i \leq 30$ kW/m, there is a slight reduction in power capture per unit width as the device widens. These results are consistent with the behaviour of motion-constrained point absorbers (Budal & Falnes 1979).

Large capture factors due to the point absorber effect are only possible if the water column motion is large. The near linear increase in power capture with device width implies that water column heave is approximately equal for all device widths tested

and thus the motion is limited by viscosity-related losses. The benefits of the point absorber effect only become evident when heave motion is limited by wave-making losses, i.e. radiation damping.

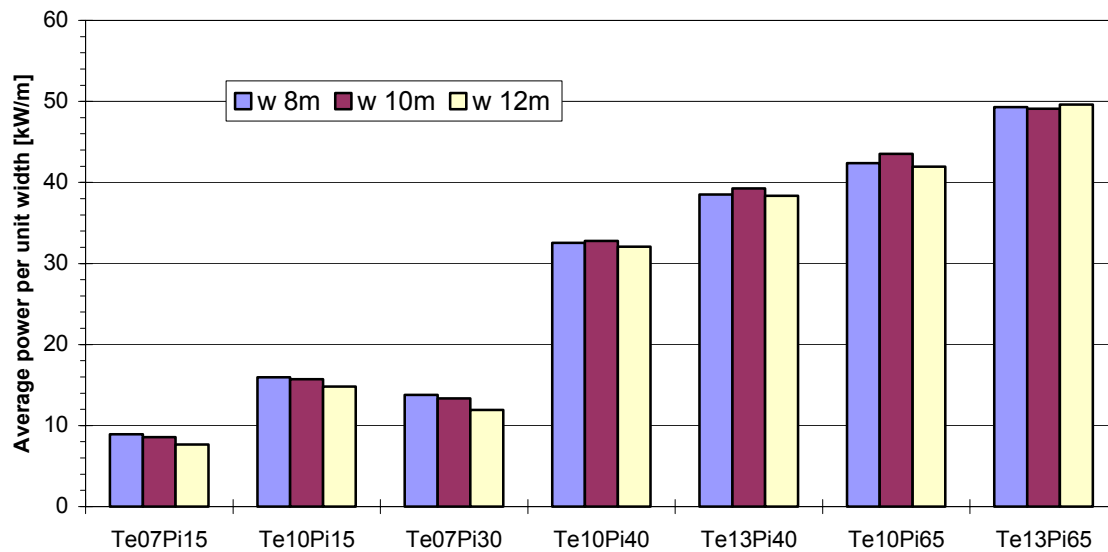


Figure 20: Influence of device width on pneumatic power capture per unit width

4.6 Comparison with narrow wave-tank tests

The use of a narrow wave-tank allows for more rapid experimentation of parameters parallel to the direction of wave propagation, with the windowed section enabling the in-plane motion of the water adjacent and within the water-column to be studied in detail. The characteristics of these motions observed in the narrow wave-tank do not appear to be any different in the wide wave-tank and thus it is reasonable for conclusions regarding the behaviour of the device to be transferred from the narrow wave-tank tests to the wide wave-tank tests.

When tested in similar seas, although the behaviour of the device shows little change, the power capture is increased in the wide wave-tank when compared to the power capture calculated from the narrow wave-tank tests. The comparisons are shown in *Figure 21*. However, these tests were performed with the model isolated within the wide wave-tank; i.e. there was no coastline beyond the short side walls on either side of the chamber.

If a solid coastline is added so that it extends over one metre either side of the model then the change in capture factor is illustrated in *Figure 22*. Except for the shorter energy period seas, there is a significant increase in power capture with the extended coastline due to it acting as a reflecting boundary. This initially appears to contradict results obtained previously and reported in “Coastline sensitivity” (Folley 2001), however, in the earlier tests the coastline integral to the model was significantly longer. The results do show however that the power capture in the wide wave-tank is significantly larger than those obtained in the narrow wave-tank. Consequently, power captures derived from narrow wave-tank results are likely to significantly underestimate the actual device performance.

The higher power captures result in a larger value for the optimum damping, together with larger water-column motion. This extra motion can cause an increase in the

incidence of water-column breaching, meaning that slightly greater lip submergence may be appropriate than that specified from the narrow wave-tank tests.

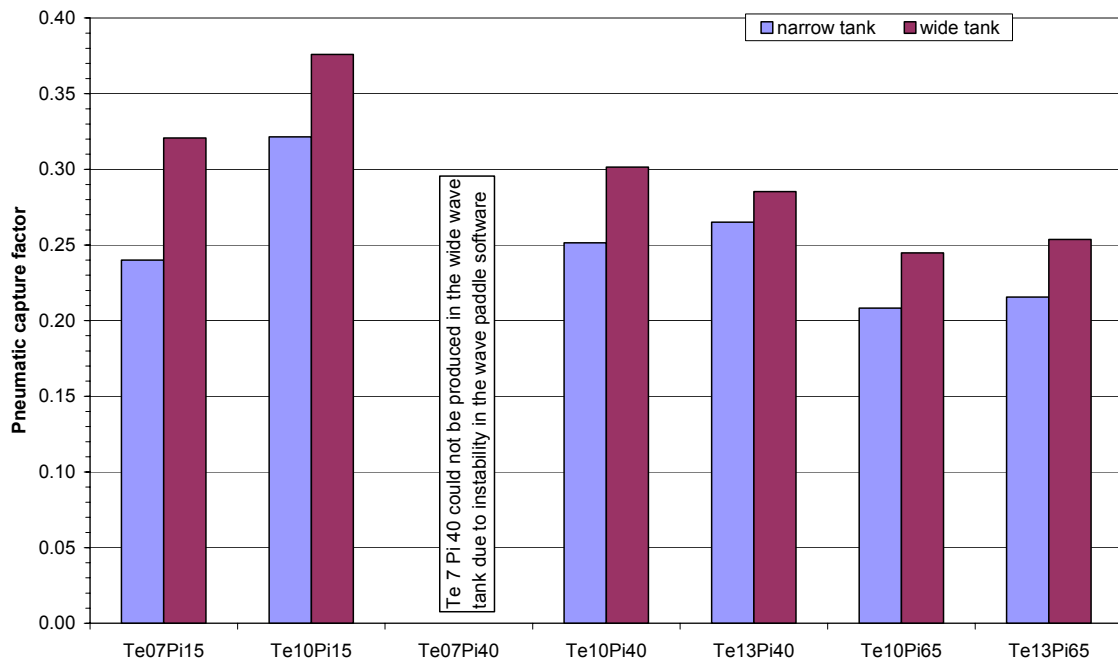


Figure 21: Comparison of narrow and wide wave-tank pneumatic capture factors

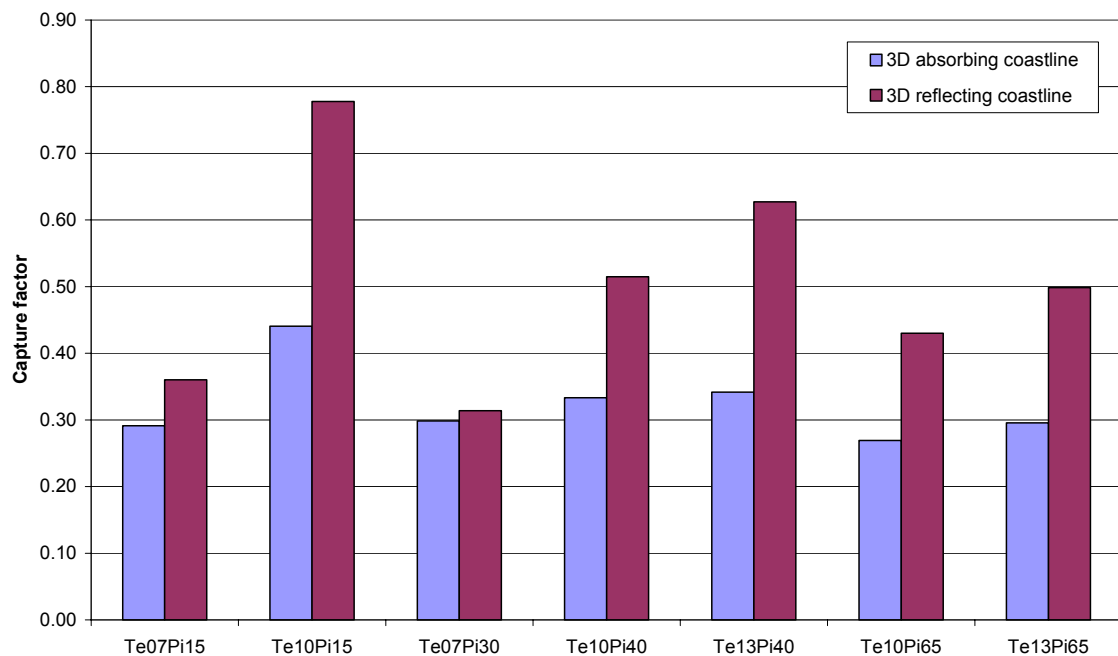


Figure 22: Comparison of capture factors with and without extended coastline

In conclusion, whilst tests performed in the narrow wave-tank are essential for developing an understanding of device performance, care must be taken in translating these results into data used for productivity analysis. The difference in performance

between the narrow and wide wave-tanks is unlikely to be a simple linear relationship and more likely to be a complex relationship between the wave-tank width and wavelength. Moreover, optimisations performed from results derived from narrow wave-tank tests must be reviewed critically to ensure that they remain valid in more realistic conditions.

4.7 Influence of wave directionality

The wide wave-tank allows the performance of a device to be tested in directionally spread seas, and with waves that are propagating obliquely to the coastline. The spreading parameters and the obliqueness of the mean wave propagation tested were chosen to represent extreme values providing upper bounds to any reduction in performance due to variations in wave directionality. An absolute measure of effect of wave directionality is more problematic due to the general lack of wave directionality data.

Although the wide wave-tank is capable of generating oblique waves, and that these waves can be explicitly specified using the wave paddle software, it is not easy to measure the actual waves generated and in particular the influence of transverse waves that develop much more readily with obliquely generated waves. This report assumes that the waves generated are equal to the waves specified, however the constraints of this assumption are included in the analysis to the extent that only general influences on performance are identified and discussed.

The effect of wave directionality on performance has a similar characteristic for all the device configurations tested. A typical effect of wave directionality is shown in *Figure 24*. These show that whilst wave directionality reduces performance, the reduction is generally less than approximately 15%.

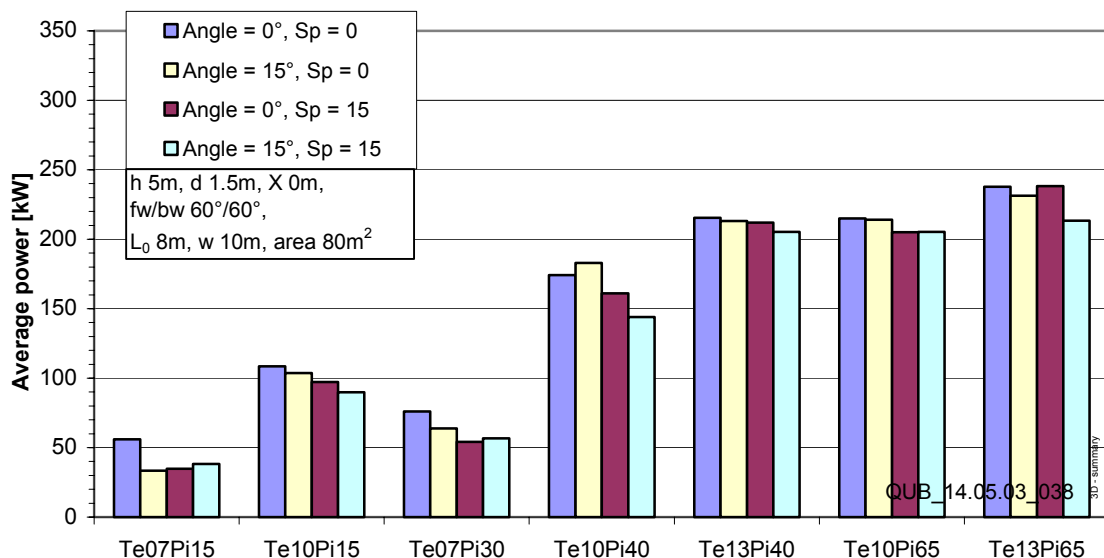


Figure 24: Effect of wave directionality on the performance of a 10 metre wide device, with a water plane length of 8 metres and in a water depth of 5 metres.

4.8 Analysis of wave energy contribution from each sea

Examination of graphs showing the power capture for each sea tested could be misleading since they contain no information about the probability of occurrence for each sea. A stretchy axis bar chart, where the width of each bar is proportional to its probability of occurrence provides this information. More conventionally, a pie chart

showing the annual energy contribution from each sea can also be used, although this does not show the power capture for each sea. The exact proportion of energy that can be attributed to each representative sea depends on the local wave climate. **Figures 25** and **26** show the energy / power capture for a 10 metre wide device, with a water plane area of 80m² using a stretchy axis bar chart and pie chart respectively, using data from Waverider buoy 62106 to provide the distribution.

These show clearly that the higher energy seas only make a small contribution to the total energy production and that the most significant sea has an energy period of 10 seconds and an incident wave power of 15 kW/m. It is often necessary when making initial design decisions to have a particular operating point, this analysis of the distribution of wave energy implies that this design point should be somewhere close to an energy period of 10 seconds and an incident wave power of 15kW/m for devices sited on the western coast of Scotland.

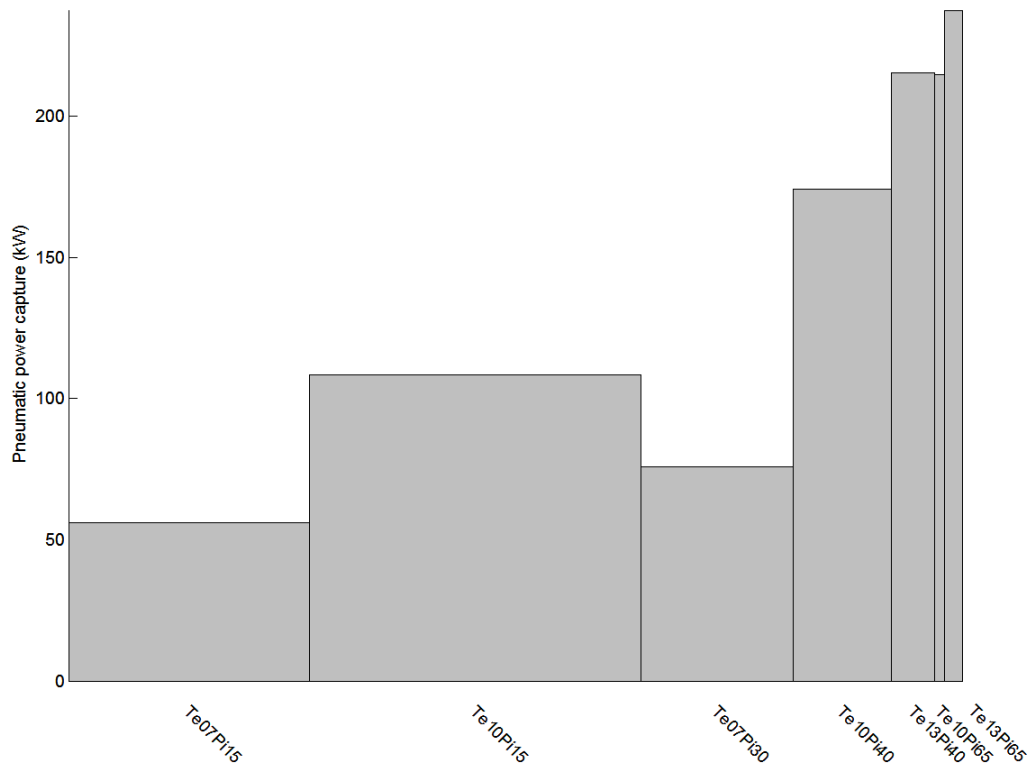


Figure 25: Stretchy-axis bar chart

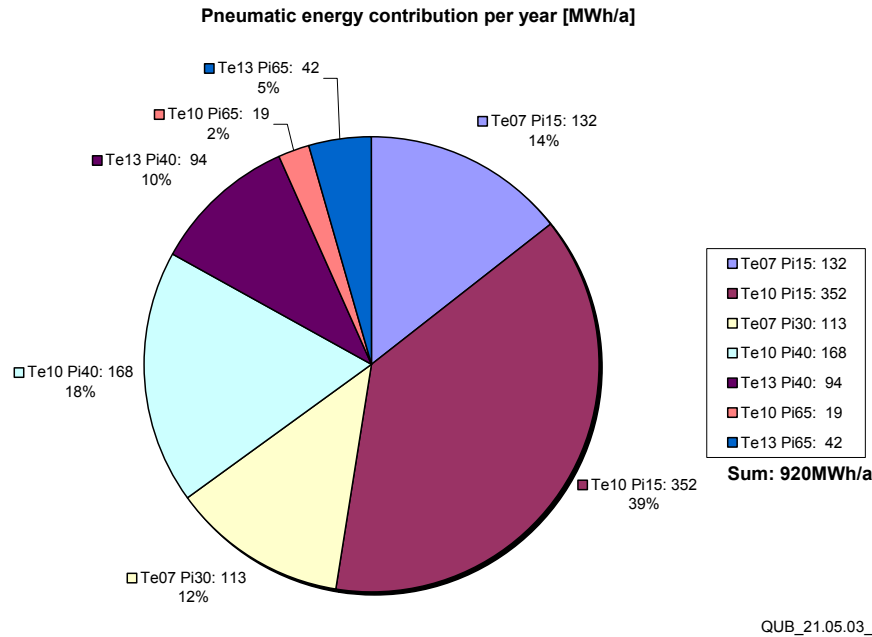


Figure 26: Pie chart for 5m water depth, 10 m device width, 80 m² water plane area

These Figures clearly illustrate the relative importance of each test sea. Thus although the power capture is higher for the more energetic seas, the most important sea with respect to average energy capture has an energy period of 10 seconds and a incident wave power of 15 kW/m.

4.9 Conclusions from 3D Testing

The following conclusions are in addition to those listed in section 3.3

1. In the range of device widths tested (7 – 12 metres) there was little evidence of transverse parasitic waves in the water column, for all seas tested.
2. Pneumatic power capture is not significantly reduced by directionally spread seas, or seas approaching at an angle to the shoreline.
3. The most significant sea with respect to productivity used in the test set had an energy period of 10 seconds and incident power of 15 kW/m. This sea is suitable as an initial design point for wave energy converters on the western coast of Scotland. The seas with 65 kW/m make only a small contribution to the average power capture.
4. Local topography should be used to improve performance cautiously since headlands/gullies have associated bathymetries that may work against perceived increases in performance.
5. In a water-depth of five metres an average pneumatic power of 1.3 kW/m² of water plane area can be obtained in the optimal configuration tested.

4.10 References

Budal K. & Falnes J. (1979). Interacting Point Absorbers With Controlled Motion. Power from sea waves, Edinburgh.

Demirbilek Z. & Vincent L. (2002). Water waves mechanics. Coastal Engineering Manual, Part II, Hydrodynamics, Chapter II-1. L. Vincent. Washington, DC., U.S.Army Corps of Engineers. **2**: 1 - 115.

Folley M. (2001) **Coastline sensitivity**, Internal report, Queens University Belfast

Stewart T. P. (1993). The Influence of Harbour Geometry on the Performance of Oscillating Water Column Wave Power Converters. Faculty of Engineering. Belfast, Queen's University Belfast.